Available online at www.sciencedirect.com
SCIENCE DIRECT®
Journal of Magnetic Resonance 171 (2004) 48–56
JMR Journal of Magnetic Resonance
www.elsevier.com/locate/jmr

Enhancing sensitivity or resolution of homonuclear correlation experiment for half-integer quadrupolar nuclei

Gregor Mali*, Venčeslav Kaučič

National Institute of Chemistry, Hajdrihova 19, SI-1001 Ljubljana, Slovenia

Received 24 June 2004
Available online 26 August 2004

Abstract

We have recently introduced double-quantum homonuclear correlation NMR experiment for half-integer quadrupolar nuclei in solids, which was based on rotary resonance recoupling [J. Chem. Phys. 120 (2004) 2835]. In this contribution we show on two ^{23}Na ($I = 3/2$) containing samples, Na_2SO_4 and Na_2HPO_4, that the efficiency of the experiment can be substantially enhanced by adding rotor assisted population transfer (RAPT) and Carr–Purcell–Meiboom–Gill (CPMG) sequences to it. We also present an upgraded two-dimensional experiment, in which double- and six-quantum coherences are correlated during t_1 evolution period, yielding a high-resolution isotropic spectrum along an indirectly detected dimension. The sensitivity of the upgraded experiment is, however, greatly reduced compared to the sensitivity of the original experiment, so that its application is feasible only when RAPT and CPMG can be used as well.

Keywords: MAS NMR; Half-integer quadrupolar nuclei; Dipolar coupling; Double quantum; Multiple quantum; CPMG

1. Introduction

Interest in solid-state nuclear magnetic resonance (NMR) spectroscopy of half-integer quadrupolar nuclei is driven by the important role that these nuclei play in many solids, such as in catalysts, semiconductors, and glasses [1,2]. In most of materials, however, the above mentioned nuclei experience strong quadrupolar interaction with surrounding electric-field gradients. In powders, this orientation dependent interaction leads to NMR lines broadened into MHz range. Although contribution to the line broadening due to first order effects can be avoided by limiting excitation to the central transition, second-order quadrupolar effects can in magnitude still be comparable to chemical shift anisotropy and dipolar coupling effects. More than that, the second-order quadrupolar anisotropy cannot be averaged out by rotating the sample about a single fixed axis, which means that, on the contrary to what happens in spin-1/2 spectroscopy, magic angle sample spinning (MAS) NMR spectroscopy of half-integer quadrupolar nuclei cannot yield high-resolution isotropic spectra. Strong quadrupolar interaction, which becomes time-dependent under MAS, also obstructs the development of advanced homo- and heteronuclear correlation techniques for half-integer quadrupolar nuclei, inevitable for structural analyses of the above described solids. Quadrupolar interaction, namely, exceeds the strength of the interaction between a nuclear spin and radiofrequency (RF) field by orders of magnitude, so that the response of a quadrupolar nucleus to RF pulses is different from the response of a spin-1/2 nucleus and most of the methods developed for spin-1/2 systems cannot be directly translated to systems of quadrupolar nuclei.

Nevertheless, within the last decade solid-state NMR spectroscopy of half-integer quadrupolar nuclei has

* Corresponding author. Fax: +386 1 47 60 300.
E-mail address: gregor.mali@ki.si (G. Mali).

1090-7807/$ - see front matter © 2004 Elsevier Inc. All rights reserved.
doi:10.1016/j.jmr.2004.08.003

developed remarkably. The problem of resolution was successfully addressed by two-dimensional multiple-quantum MAS (MQMAS) technique[3], which correlates evolution of multiple-quantum coherences and single-quantum central-transition coherence under MAS, yielding refocusing of second-order quadrupolar effects. Alternatively, refocusing can be achieved also by correlating single-quantum satellite-transition and central-transition coherences using the so called satellite-transition MAS (STMAS) technique[4]. Two-dimensional MQMAS and STMAS spectroscopies both provide high-resolution isotropic spectra along one of the two dimensions.

A possible approach to the development of homo- and heteronuclear correlation techniques for half-integer quadrupolar nuclei is through application of weak (selective) RF fields, which affect only central-transition coherence and leave satellite-transition coherences intact. Such a restriction allows one to describe half-integer quadrupolar nuclei as fictitious spins 1/2. Consequently, in experiments, in which weak RF pulses are employed, behavior of half-integer quadrupolar and spin-1/2 nuclei is expected to be similar. Very recently, indeed, a two-dimensional double-quantum homonuclear correlation technique for half-integer quadrupolar nuclei was introduced [5,6], which was based on a HOR-ROR experiment [7] designed for dipolar-coupled spin-1/2 nuclei. (The technique was termed DQ-DCQ, which stands for double-quantum experiment for dipolar-coupled quadrupolar nuclei [8].) The proposed technique was successfully tested on two samples containing spin-3/2 and spin-5/2 quadrupolar nuclei, respectively. The appearance of detected two-dimensional spectra was similar to the appearance of double-quantum spectra of coupled spin-1/2 nuclei, except that NMR signals of half-integer quadrupolar nuclei were in both dimensions broadened by the second-order quadrupolar effects. When nuclear sites in a material under study were characterized by large quadrupolar coupling constants and small differences in isotropic chemical shift, extensive overlap of NMR signals made an analysis of homonuclear correlation spectra very difficult. To circumvent this problem, we present here an upgraded two-dimensional homonuclear correlation experiment for half-integer quadrupolar nuclei, which yields high-resolution isotropic spectrum along an indirectly detected dimension. In a similar way as split-t_1 MQMAS experiment[9] correlates single-quantum and triple-quantum coherences during t_1 evolution period to refocus second-order quadrupolar effects just before the acquisition period t_2, the proposed experiment correlates two-spin double-quantum and six-quantum coherences.

Because the excitation of six-quantum (6Q) coherences is quite inefficient, in this contribution we first discuss possibilities on how to enhance the signal of either the original or the modified homonuclear correlation experiment. In both two-dimensional experiments the preparation period comprises excitation of two-spin double-quantum (2Q) coherences from central-transition magnetization. One may therefore expect that selective saturation of satellite transitions by a train of RF pulses, which enhances the population difference across the central transition, can effectively enlarge sensitivity of experiments. Application of such a train of pulses is termed rotor assisted population transfer (RAPT) [10]. It theoretically enables enhancement by a factor of $I + 1/2$, where I is the spin quantum number. In practice enhancement factors of about 1.8 were observed for nuclei with $I = 3/2$. Even larger sensitivity gain can be obtained by modifying the detection periods of experiments with quadrupolar version of Carr–Purcell–Meiboom–Gill (CPMG) sequence [11]. In this approach, instead of recording a single free-induction-decay, a train of selective refocusing π pulses is applied within the detection period, yielding a series of echoes. Fourier transformation of this series splits a second-order quadrupolar MAS lineshape into a number of spin-echo sidebands and thus enhances a signal in a similar way as MAS enhances a signal by splitting a static quadrupolar lineshape into a number of spinning sidebands.

2. Experimental

All measurements were performed on Varian Unity Inova spectrometer with a 14.1 T narrow-bore magnet and a 5 mm Doty MAS probehead. In all measurements samples were rotated at 12.5 kHz. Pulse sequences for homonuclear correlation spectroscopy, which are described in details in the following sections, were tested on anhydrous Na_2SO_4 and anhydrous Na_2HPO_4. Sodium nuclei within Na_2SO_4 occupy a single crystallographic site characterized by $C_Q = 2.6$ MHz and $\eta_Q = 0.6$ [12]. There are three inequivalent sodium crystallographic sites within Na_2HPO_4, Na_1 with $C_Q = 2.0$ MHz and $\eta_Q = 0.7$, Na_2 with $C_Q = 1.4$ MHz and $\eta_Q = 0.2$, and Na_3 with $C_Q = 3.7$ MHz and $\eta_Q = 0.3$ [13]. Distances among nearest sodium neighbors within both materials are listed in Table 1. The above-listed quadrupolar parameters were used also in numerical simulations, which were carried out by SIMPSON [14].

Table 1
Distances (in Å) among nearest sodium neighbours in Na_2SO_4 and Na_2HPO_4

Na_2SO_4	Na	Na_2HPO_4	Na_1	Na_2	Na_3
Na	3.21	Na_1	5.45	3.42	3.41
		Na_2	3.42	5.45	3.31
		Na_3	3.41	3.31	3.90

3. Enhancing signal by RAPT and CPMG

We first compare the performance of the original 2Q homonuclear correlation experiment with experiments that employ RAPT and CPMG sequences. The corresponding three pulse sequences are schematically presented in Fig. 1. The original 2Q experiment starts with a spin-lock pulse that is preceded and followed by selective π/2 pulses. If the amplitude of the RF field during the spin-lock pulse satisfies the rotary resonance condition

$$\left(I+\frac{1}{2}\right)\nu_{RF}=\frac{1}{2}\nu_R, \tag{1}$$

average Hamiltonian corresponding to an on-resonance bracketed spin-lock pulse contains only 2Q spin-operator terms and thus efficiently excites 2Q coherences [6]. Here $\nu_{RF}=\gamma B_{RF}$ and ν_R is frequency of sample rotation. Phase of the spin-lock pulse can be shifted by π in the middle of the pulse, so that single-quantum terms, which may appear due to offset effects, still vanish from the average Hamiltonian. A selective π pulse at the beginning of t_1 evolution period differentiates coherence transfer pathways of 2Q coherences arising from dipolar-coupled spins and from a single spin, so that the latter can be efficiently filtered out by phase cycling. The two-spin 2Q coherences are then allowed to evolve for time t_1 before they are converted to 0Q coherence with a second bracketed spin-lock pulse. The signal is acquired after a selective π/2 pulse.

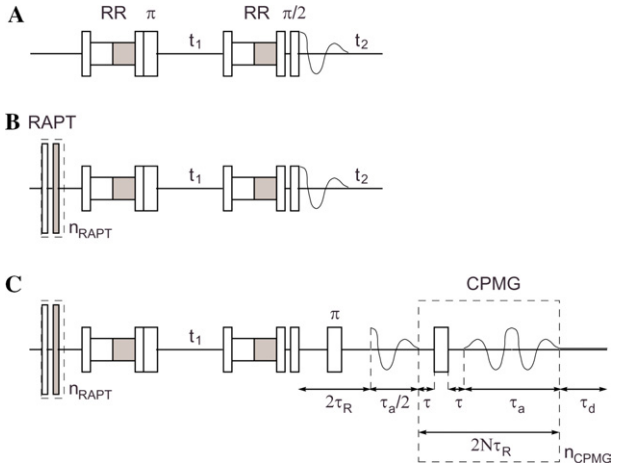

Fig. 1. Pulse sequences for 2Q homonuclear correlation experiment on half-integer quadrupolar nuclei: (A) the original scheme, (B) scheme with RAPT, and (C) scheme with RAPT and CPMG. All schemes use bracketed spin-lock pulses for the excitation of 2Q coherences and for their conversion to 0Q coherences. RF field during spin-lock satisfies rotary-resonance condition. All pulses except pulses within RAPT sequence are central-transition selective pulses. Basic RAPT block, built of two delays and two pulses whose RF phase differ by π, is repeated n_{RAPT} times. CPMG block consists of a selective refocusing π pulse and τ_a long acquisition interval. After the block is repeated n_{CPMG} times an acquisition period of τ_d allows the last spin-echo to decay completely.

RAPT sequence, added at the beginning of the original pulse scheme to selectively saturate satellite transitions, is composed of a train of strong and short pulses separated by short delays. The basic block that is repeated n_{RAPT} times can be described with a τ_p–τ_w–τ_p–τ_w sequence, where τ_p stands for the pulse length and τ_w stands for the duration of a delay (window). The phase of the second pulse is shifted by π with respect to the phase of the first pulse. For optimal performance the duration of the complete train of pulses and delays should be about one rotation period [10]. The duration of one block determines the modulation frequency of this amplitude-modulated RF scheme, $1/\nu_m = 2(\tau_p + \tau_w)$. To achieve maximal enhancement, modulation frequency should be on the order of $C_Q/4$ [10], where C_Q is quadrupolar coupling constant. For RAPT sequences in all our experiments, however, τ_p and τ_w were both fixed to 1 μs, yielding ν_m of 250 kHz. The duration of the entire modulation scheme was exactly one rotor period and maximal available ν_{RF} of about 60 kHz was used.

CPMG sequence replaces the usual detection period at the end of a pulse sequence. A selective π pulse preceding CPMG refocuses ±1Q coherences, which are generated by the readout pulse of the original experiment, and allows one to start acquisition exactly on top of spin echo. The sequence is rotor-synchronized according to $2N\tau_R = \tau_a + 2\tau + \tau_\pi$, where $2N$ is a number of rotor echoes per spin-echo period, τ_R is rotation period, τ_a is an acquisition interval, and τ is a short delay preceding and following the refocusing π pulse (τ_π) [11]. After the CPMG sequence an acquisition period of τ_d is added to allow spin echo to decay completely.

One-dimensional ^{23}Na spectra and corresponding time-domain signals, recorded in Na_2SO_4 with the above-described pulse sequences, are compared in Fig. 2. RAPT enhances central-transition signal by a factor of 1.8 and CPMG improves the signal-to-noise ratio by an additional factor of 3.3. The total sensitivity gain of a pulse sequence that uses both RAPT and CPMG is thus about a factor of 6. Actually, CPMG can lead to a large gain in signal-to-noise ratio only when inhomogeneous decay is much faster than the homogeneous one [15]. In Na_2SO_4 the difference in both decay rates is not so prominent and several spin echoes, required to noticeably improve the signal-to-noise ratio, were detected only when the acquisition interval τ_a was short enough—about 3 ms or less. There are two consequences associated with short acquisition intervals. First, the resulting spectrum is split into spin-echo sidebands that are separated by $1/\tau_a$. Thus, if τ_a is small, the separation between sidebands is large and only few sidebands represent the original second-order quadrupolar lineshape. Second, if the acquisition interval is too short, spin-echo can be truncated, the envelope of spin-echo sidebands in the spectrum can become distorted and can thus no longer faithfully reflect the second-order quadrupolar lineshape. Obviously,

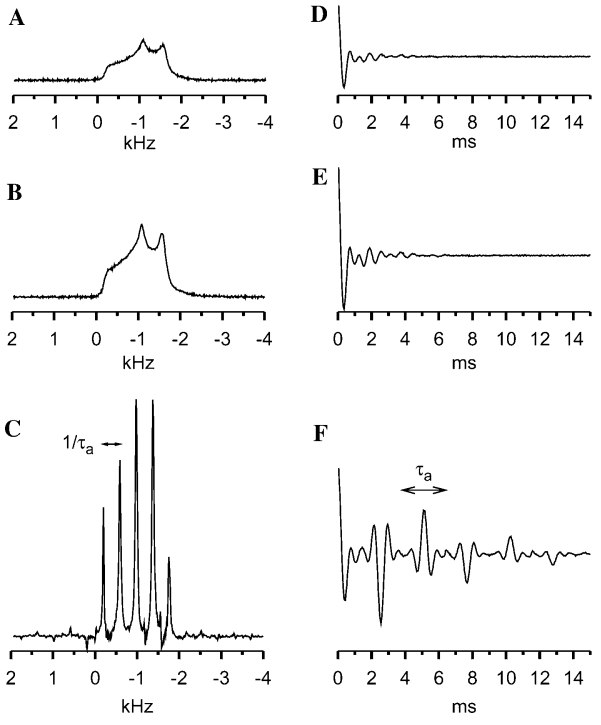

Fig. 2. One-dimensional ^{23}Na spectra and corresponding time-domain signals recorded in Na_2SO_4 with different 2Q homonuclear correlation pulse sequences—(A and D) original sequence, (B and E) sequence with RAPT, (C and F) sequence with RAPT and CPMG. In all experiments sample was rotated at 12.5 kHz, the number of scans was 32 and repetition delay was 4 s. RAPT block was 4 μs long and was repeated 20 times. CPMG block was determined by $\tau = 58$ μs, $\tau_\pi = 44$ μs, and $\tau_a = 2560$ μs. It was repeated 10 times.

while RAPT is a robust block that can safely be employed to increase the central-transition signal, the performance of CPMG can depend much on the sample and may be acceptable mostly when details about second-order quadrupolar lineshapes are not very important.

4. Enhancing resolution by 2Q6Q correlation experiment

Second-order quadrupolar broadening limits the resolution of the above presented homonuclear correlation experiments and makes analysis of recorded two-dimensional spectra difficult. A possible way to remove quadrupolar broadening at least along one dimension is to use a split-t_1 experiment in which 2Q coherences are correlated with 6Q coherences. For a coupled pair of spin-3/2 nuclei, the evolution of the density matrix in such an experiment can be schematically outlined as

$$\begin{aligned} I_z^{23} + S_z^{23} &\rightarrow I_+^{23} S_+^{23} \mathrm{e}^{-\mathrm{i}\left(\nu_I^{\mathrm{CT}} + \nu_S^{\mathrm{CT}}\right) k t_1} \\ &\rightarrow I_+^{14} S_+^{14} \mathrm{e}^{-\mathrm{i}\left(\nu_I^{\mathrm{CT}} + \nu_S^{\mathrm{CT}}\right) k t_1} \mathrm{e}^{-\mathrm{i}\left(\nu_I^{3\mathrm{Q}} + \nu_S^{3\mathrm{Q}}\right)(1-k) t_1} \\ &\rightarrow \left(I_-^{23} \mathrm{e}^{\mathrm{i}\nu_I^{\mathrm{CT}} t_2} + S_-^{23} \mathrm{e}^{\mathrm{i}\nu_S^{\mathrm{CT}} t_2} \right) \mathrm{e}^{-\mathrm{i}\left(k\left(\nu_I^{\mathrm{CT}} + \nu_S^{\mathrm{CT}}\right) + (1-k)\left(\nu_I^{3\mathrm{Q}} + \nu_S^{3\mathrm{Q}}\right)\right) t_1}. \end{aligned} \tag{2}$$

Here I_+^{23}, S_+^{23} are fictitious spin-1/2 operators associated with 1Q central-transition coherences and I_+^{14}, S_+^{14} are fictitious spin-1/2 operators associated with 3Q coherences. Bilinear terms, $I_+^{23} S_+^{23}$ and $I_+^{14} S_+^{14}$, represent two-spin 2Q and 6Q coherences, respectively. Each step in the above expression comprises an excitation/conversion followed by an evolution that is governed by second-order quadrupolar interaction. In the first step of the proposed homonuclear correlation experiment, as in the original 2Q experiment, two-spin 2Q coherence is generated from central-transition magnetization. The 2Q coherence is allowed to evolve for time kt_1 before it is transferred to 6Q coherence. Evolution of the former under the quadrupolar interaction introduces oscillations characterized by a sum of orientation-dependent central-transition frequencies ν_I^{CT} and ν_S^{CT}. Orientation dependence of $\nu_{I,S}^{\mathrm{CT}}$ is responsible for line broadening, observed when the original 2Q homonuclear correlation experiment is applied to a powdered sample. After the excitation of 6Q coherence, the latter evolves under the quadrupolar interaction for a period of $(1-k)t_1$ and is then converted to observable -1Q coherence. The evolution of 6Q coherence is described with a sum of orientation-dependent 3Q transition frequencies $\nu_I^{3\mathrm{Q}}$ and $\nu_S^{3\mathrm{Q}}$. Selection of a proper k can cause the angular-dependent parts of $\nu_{I,S}^{\mathrm{CT}}$ to cancel with angular-dependent parts of $\nu_{I,S}^{3\mathrm{Q}}$ at the end of t_1 evolution period [3]. For dipolar-coupled pair of spin-3/2 nuclei selection of $k = 7/16$ [9] thus leads to a signal that is broadened by second-order quadrupolar effects in directly detected dimension but isotropic in indirectly detected dimension

$$\begin{aligned} s(t_1, t_2) &= s(0) \left(\mathrm{e}^{\mathrm{i}\nu_I^{\mathrm{CT}} t_2} + \mathrm{e}^{\mathrm{i}\nu_S^{\mathrm{CT}} t_2} \right) \mathrm{e}^{-\mathrm{i}\left(k\left(\nu_I^{\mathrm{CT}} + \nu_S^{\mathrm{CT}}\right) + (1-k)\left(\nu_I^{3\mathrm{Q}} + \nu_S^{3\mathrm{Q}}\right)\right) t_1} \\ &= s(0) \left(\mathrm{e}^{\mathrm{i}\nu_I^{\mathrm{CT}} t_2} + \mathrm{e}^{\mathrm{i}\nu_S^{\mathrm{CT}} t_2} \right) \mathrm{e}^{-\mathrm{i}\left(\nu_I^{\mathrm{iso}} + \nu_S^{\mathrm{iso}}\right) t_1}. \end{aligned} \tag{3}$$

To shorten mathematical expressions the above discussion was limited to a single coherence transfer pathway, $0 \rightarrow 2 \rightarrow 6 \rightarrow -1$. If experiment comprises also a mirror pathway $0 \rightarrow -2 \rightarrow -6 \rightarrow -1$ and if conversion from $\pm$6Q coherences to -1Q coherence passes through a z-filter, symmetric pathways will produce an amplitude modulated signal along indirectly detected dimension and thus lead to pure absorption two-dimensional spectrum [16].

The actual pulse scheme of the above-proposed 2Q6Q homonuclear correlation experiment is compared to pulse sequences of the original 2Q homonuclear correlation and split-t_1 3QMAS experiments in Fig. 3. The experiment starts with excitation of $\pm$2Q coherences through a bracketed spin-lock pulse. Transfer from $\pm$2Q to $\pm$6Q coherences, i.e., conversions $I_\pm^{23} \rightarrow I_\pm^{14}$ and $S_\pm^{23} \rightarrow S_\pm^{14}$, can be achieved in several ways, by RIACT [17], FASTER [18], FAM [19] or CW [20] pulse. As we shall show below by numerical simulations and experimental results, with available ν_{RF} of about

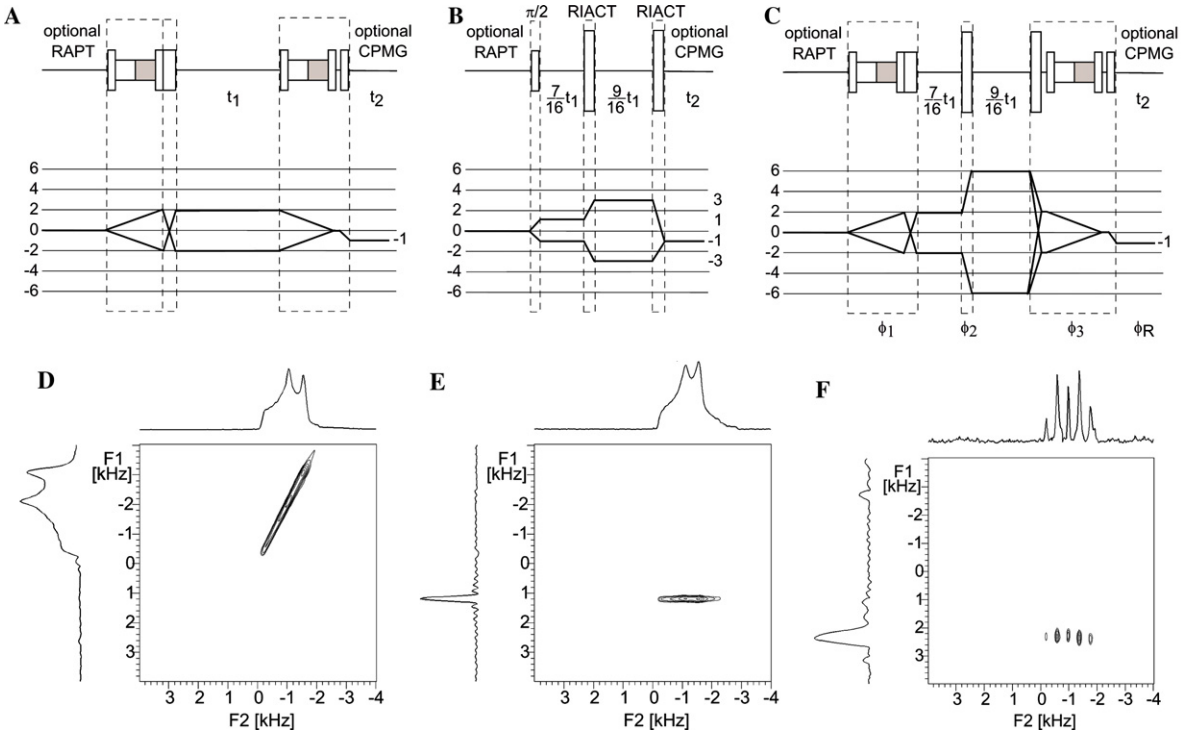

Fig. 3. Comparison of high-resolution 2Q6Q homonuclear correlation experiment for spin-3/2 nuclei with related 2Q homonuclear correlation and split-t_1 3QMAS experiments. Pulse sequences and coherence transfer pathways for 2Q, 3Q, and 2Q6Q experiments are shown in (A–C), respectively. Corresponding two-dimensional ^{23}Na spectra recorded in Na_2SO_4 are presented in (D–F). In 2Q, 3Q, and 2Q6Q experiments number of scans was 32, 48, and 384, respectively, repetition delay was 1, 0.6, and 4 s, respectively, and number of increments along t_1 was 40, 60, and 20, respectively. All RIACT pulses were 60 μs long ($3\tau_R/4$). Parameters for RAPT and CPMG sequences, employed within a 2Q6Q homonuclear correlation experiment, were equal to those used in one-dimensional experiments presented in Fig. 2. In all experiments acquisition along indirectly detected dimension was synchronized with rotation and hypercomplex approach was used.

60 kHz RIACT approach is the most efficient. Conversion of ±6Q coherences to detectable −1Q coherence is a three-step process consisting of a RIACT pulse (±6Q → ±2Q), a bracketed spin-lock (±2Q → 0Q), and a selective π/2 pulse (0Q → −1Q).

It should be noted here that relatively recently a different 6Q-filtered homonuclear correlation experiment for spin-3/2 nuclei was presented [21]. As opposed to the proposed 2Q6Q experiment, the 6Q experiment does not yield isotropic spectra. It uses a single strong pulse to excite 6Q coherence and after an evolution period of t_1 another strong pulse to covert it to −1Q coherence. The experiment thus relies on the property, that due to the presence of strong quadrupolar interaction MAS cannot average out the dipolar coupling completely. In principle therefore no recoupling scheme is needed for generation of two-spin 2Q or 6Q coherences in systems of coupled quadrupolar nuclei [21,22]. However, though feasible, such 2Q or 6Q coherence excitation is much less efficient than the excitation that uses rotary-resonance recoupling [6]. The drawback of the latter approach is only that sufficiently weak RF fields have to be used to ensure that quadrupolar nuclei behave in a similar way as spin-1/2 nuclei.

The feasibility of 2Q6Q homonuclear correlation experiment was first tested on Na_2SO_4. The corresponding two-dimensional spectrum is shown in Fig. 3. It is useful to compare it to the spectra obtained with the original 2Q experiment and with the split-t_1 3QMAS experiment. 2Q homonuclear correlation spectrum exhibits a single strong peak confirming that there is a single crystallographically distinct sodium site within Na_2SO_4 and that ^{23}Na nuclei occupying neighboring positions within a crystal are quite strongly dipolar coupled. The peak in the two-dimensional spectrum is, however, broadened by the second-order quadrupolar anisotropy and its width along the indirectly detected (double-quantum) dimension is twice as large as its width along the directly detected dimension. The 3QMAS spectrum exhibits a narrow isotropic projection onto the indirectly detected dimension, but of course, does not provide information on the dipolar coupling. The corresponding split-t_1 experiment was performed by first exciting ±1Q coherences by a selective π/2 pulse, by letting them evolve for a period of $7t_1/16$, converting them to ±3Q coherences by the first RIACT pulse, allowing these to evolve for a period of $9t_1/16$ and finally converting them to detectable −1Q coherence by the second RIACT pulse. Spectrum of the new 2Q6Q experiment combines prop-

erties of both above-mentioned experiments—it exhibits a signal of dipolar-coupled ^{23}Na nuclei, which is isotropic along the indirectly detected dimension. The isotropic signal is not as narrow as is the signal of the 3QMAS spectrum, which might be due to faster decay of 2Q and 6Q coherences as compared to the decay of 1Q and 3Q coherences. Nevertheless, the 2Q6Q homonuclear correlation experiment still promises much better resolution than the original 2Q experiment.

The two-dimensional 2Q6Q spectrum was recorded in 15 h. Compared to the 2Q homonuclear correlation experiment, 2Q6Q experiment was much less efficient and in order to complete it in a reasonable amount of time an application of RAPT and CPMG was inevitable. A 384-step nested phase cycling with $\phi_1 = k_1\frac{2\pi}{4}$, $\phi_2 = k_2\frac{2\pi}{8}$, $\phi_3 = k_3\frac{2\pi}{12}$, and $\phi_R = (k_1 + k_2)\pi - k_3\frac{5\pi}{6}$ was used to select $0 \to \pm 2 \to \pm 6 \to -1$ coherence transfer pathway. In fact the above phase cycling selects also $0 \to \pm 6 \to \mp 6 \to -1$ pathway, which can, however, safely be ignored, because the probability of exciting 6Q coherences with selective bracketed spin-lock pulse is negligible. Though the phase cycle is very long, one has to remember that the experiment itself is also quite insensitive so that at least 384 free-induction decays usually need to be co-added to ensure a reasonable signal-to-noise ratio. If sensitivity of experiment was larger and not as many repetitions were needed for signal-to-noise ratio reasons, cogwheel phase cycling [23] could be used instead. The shortest cogwheel cycle [24] that selects only $0 \to \pm 2 \to \pm 6 \to -1$ coherence transfer pathways and rejects all other pathways in the range of $-6Q$ to 6Q coherences requires only 64 steps, which is 1/6 of the number of steps of the nested phase cycle. Such a cogwheel phase cycle might, however, be difficult to implement on some spectrometers, because it requires RF phase changes in steps of even and odd multiples of $2\pi/64$ (5.625°). Nevertheless, even if a cogwheel cycle with a larger number of steps is chosen [25], for example a cycle with 90 steps, for which RF phases are incremented in steps of even and odd multiples of $2\pi/90$ (4°), its length is still much smaller than the length of the nested cycle. By allowing a pathway additional to $0 \to \pm 2 \to \pm 6 \to -1$, for example a pathway $0 \to \pm 5 \to \pm 5 \to -1$ that can again be neglected, even shorter and more spectrometer-friendly cogwheel phase cycles can be found. One example is a 40-step cycle denoted by COG40(28,1,0;20), for which RF phases in the first block of pulses are incremented in steps of 252°, phase of the first RIACT pulse is incremented in steps of 9°, phases of the third block of pulses are fixed to 0, and receiver phase is incremented in steps of 180°.

From sensitivity point of view, the bottleneck of 2Q6Q homonuclear correlation experiment are $2Q \leftrightarrow 6Q$ coherence conversions, or in other words, simultaneous $I^{23}_{\pm} \leftrightarrow I^{14}_{\pm}$ and $S^{23}_{\pm} \leftrightarrow S^{14}_{\pm}$ conversions. It is possible to learn much about the efficiency of the experiment by studying $3Q \to 1Q$ coherence conversion ($I^{14}_{+} \to I^{23}_{+}$ mixing) only. By using numerical simulations the efficiency of such 3Q mixing was compared for CW (nutation), FASTER (rotary resonance), RIACT, and FAM approach. Results presented in Fig. 4 show that within the limits set by $0 \leqslant \nu_{RF} \leqslant 60$ kHz, RIACT mechanism is slightly more efficient than FASTER mechanism at $\nu_{RF} = 2\nu_R$ or FAM mechanism at $\nu_{RF} = 60$ kHz. The efficiency of RIACT in the maximum is 0.22. Here the efficiency of $I^{14}_{+} \to I^{23}_{+}$ mixing is defined as the ratio $|\langle I^{23}_{+}\rangle|/|\langle I^{23}_{+}\rangle|_{max}$ with theoretical maximum of $|\langle I^{23}_{+}\rangle|_{max} = 1$ [18]. Experimental results presented in Fig. 5 agree well with results of numerical simulations and also suggest that RIACT should be a scheme of

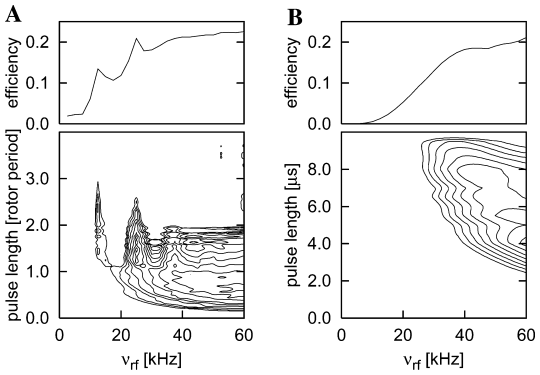

Fig. 4. Efficiency of 3Q ($I^{14}_{+} \to I^{23}_{+}$) mixing as obtained by numerical simulations. Two-dimensional contour plots show $|\langle I^{23}_{+}\rangle|$ as a function of RF-field strength and pulse length. (A) A single pulse was used for conversion, resulting in either nutation (short pulse), rotary-resonance (ν_{RF} small integer multiple of rotation frequency) or RIACT mechanism of 3Q mixing. (B) Four FAM blocks were used for conversion. Above each contour plot a skyline projection shows the maximal signal possible at each RF-field strength. Quadrupolar parameters in simulations corresponded to parameters characterizing ^{23}Na nuclei within Na_2SO_4 and rotation frequency of 12.5 kHz was assumed. RF-field strength was incremented in steps of 2.5 kHz and pulse length was incremented in steps of 5 μs in (A) and in steps of 0.5 μs in (B).

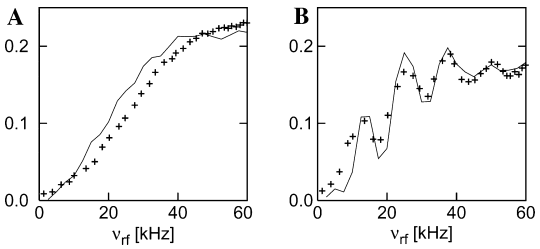

Fig. 5. Comparison of experimental results and results of numerical simulations for the efficiency of 3Q mixing using either RIACT (A) or rotary-resonance (B) mechanism. Parameters for simulations are equal to parameters described in Fig. 4. Length of a RIACT pulse was 60 μs ($0.75\tau_R$) and length of a rotary-resonance pulse was 104 μs ($1.3\tau_R$). Experimental results were not normalized by an additional experiment but all scaled by the same factor to achieve the best agreement between experimental and simulated efficiency.

choice within the 2Q6Q homonuclear correlation experiment.

Total efficiency of the 2Q6Q experiment is proportional to the forth power of the efficiency of 3Q mixing. There are namely two steps, $2Q \rightarrow 6Q$ excitation and $6Q \rightarrow 2Q$ conversion, in which dipolar-coupled spins I and S have to undergo the $1Q \rightarrow 3Q$ or $3Q \rightarrow 1Q$ transition simultaneously. This explains why sensitivity of 2Q6Q homonuclear correlation experiment is so poor, but also opens up the way to still improve it slightly. By pushing the efficiency of the 3Q mixing to 0.3, which is attainable by RIACT at ν_{RF} of 100 kHz and moderate ν_R of 10–20 kHz [18], the total sensitivity of the experiment would be multiplied by a factor of $(0.3/0.22)^4 \approx 3.5$. Such an enhancement is already comparable to the enhancement obtained by CPMG and it is certainly not negligible. Moreover, using stronger RF fields FAM approach could yield even higher efficiency than RIACT [19].

5. Homonuclear correlation experiments on Na_2HPO_4

Performance of the above-described homonuclear correlation experiments was tested also on anhydrous Na_2HPO_4. ^{23}Na MAS spectrum of this material shows (Fig. 6) that central-transition signals broadened by the second-order quadrupolar anisotropy overlap severely, which suggests that for studying proximities between sodium nuclei within Na_2HPO_4 the 2Q6Q homonuclear correlation experiment might be favorable than the original 2Q experiment. However, since quadrupolar coupling constants for sodium sites Na_1, Na_2, and Na_3 differ noticeably, efficiency of $2Q \leftrightarrow 6Q$ coherence conversions might also differ substantially, causing the signal amplitudes within two-dimensional 2Q6Q spectrum not to depend only on strength of dipolar coupling and thus on internuclear distances, but also on quadrupolar coupling constants of dipolar-coupled sodium nuclei. This assumption is supported by numerically simulated 3Q mixing experiments (Fig. 6), which show that optimal mixing efficiencies obtained by RIACT for sites Na_1, Na_2, and Na_3 are 0.25, 0.27, and 0.15, respectively.

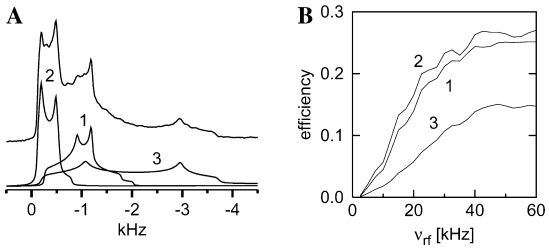

Fig. 6. Experimental MAS NMR spectrum of anhydrous Na_2HPO_4 (A) and numerically simulated RIACT 3Q mixing efficiencies for three crystallographically distinct sodium sites of this material (B). (A) The individual lines obtained by the decomposition of the recorded MAS spectrum are shown as well. Parameters for numerical simulations (B) were equal to parameters used for simulations presented in Fig. 4, except for parameters describing quadrupolar coupling.

Two-dimensional spectra of the three related experiments, 2Q homonuclear correlation, 3QMAS, and 2Q6Q homonuclear correlation experiment, are presented in Fig. 7. Analysis of 2Q homonuclear correlation spectrum is indeed difficult. Whereas broad peaks corresponding to pairs of coupled spins Na_1–Na_3, Na_2–Na_3, and Na_3–Na_3 are partly resolved, peaks that correspond to Na_1–Na_1, Na_1–Na_2, and Na_2–Na_2 pairs are entirely overlapped with each other and with aforementioned peaks. Only precise numerical simulation of the experiment might allow one to extract amplitudes of individual contributions.

On the opposite, a split-t_1 3QMAS experiment is able to resolve three contributions of sodium nuclei along an indirectly detected dimension, even though the isotropic positions of Na_1 and Na_2 signals differ by only 250 Hz. The 3QMAS spectrum of Na_2HPO_4 is useful because it allows us to extract isotropic positions of the three sodium signals and thus to predict resonance frequencies of all potential correlation peaks within 2Q6Q homonuclear correlation spectrum. Isotropic shifts of 0.52, 0.77, and 3.31 kHz for Na_2, Na_1, and Na_3 sites, respectively, predict

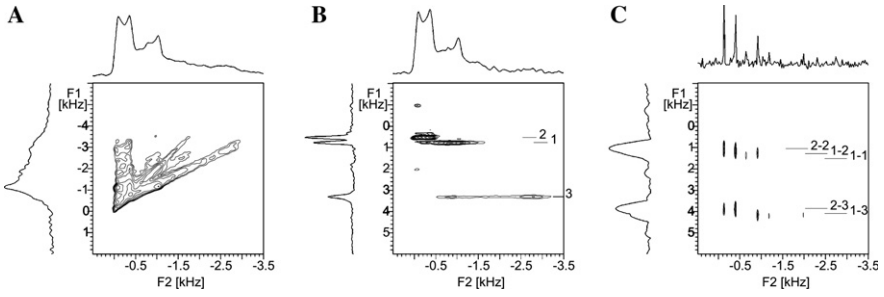

Fig. 7. Comparison of ^{23}Na 2Q homonuclear correlation, split-t_1 3QMAS and 2Q6Q homonuclear correlation spectra recorded in anhydrous Na_2HPO_4. Experiments and experimental details, except for repetition delays, number of scans and number of increments along t_1, were equal to those described in Fig. 3. Number of scans for the three experiments were 16, 48, and 1536, respectively, and number of increments were 60, 80, and 20, respectively. Repetition delay was 2 s for all experiments.

appearance of homonuclear-correlation signals of Na_2–Na_2, Na_1–Na_2, Na_1–Na_1, Na_2–Na_3, Na_1–Na_3, and Na_3–Na_3 at 1.04, 1.29, 1.54, 3.83, 4.08, and 6.62 kHz, respectively. All shifts in the spectra are given relative to the center of the spectrum, i.e., zero along the directly detected dimension is determined by the carrier frequency.

Within the recorded high-resolution 2Q6Q homonuclear correlation spectrum one can indeed detect 5 out of 6 predicted signals. The signal-to-noise ratio of the spectrum that was recorded in 30 h is acceptable and spin-echo sidebands within the projection of the spectrum onto directly detected dimension represent MAS lineshape well. Resolution, though not as good as in the 3QMAS spectrum, has improved tremendously as compared to the resolution of the 2Q homonuclear correlation spectrum. In the two-dimensional spectrum we can clearly resolve correlation peaks that correspond to Na_2–Na_2 and Na_1–Na_2 pairs. As expected the Na_2–Na_2 signal is very strong although the sodium nuclei that occupy nearest Na_2 sites are more than 5 Å apart and thus dipolar coupling between them is correspondingly small. But quadrupolar coupling constant for site 2 is the smallest among all three constants and efficiency of $2Q \leftrightarrow 6Q$ coherence conversions for this site is therefore the largest.

We can also clearly resolve correlation peaks that describe Na_1–Na_3 and Na_2–Na_3 coupling. Only dipolar coupling between two nearest Na_3 nuclei, which are 3.9 Å apart, is not detected. Clearly the efficiency of $2Q \leftrightarrow 6Q$ coherence conversions for this site was too small to yield a measurable signal. To detect it either a larger number of scans or, preferably, higher RF fields during $2Q \leftrightarrow 6Q$ conversions should be used.

6. Conclusions

Application of RAPT and CPMG sequences can in favorable cases enhance the sensitivity of 2Q homonuclear correlation experiment for half-integer quadrupolar nuclei by an order of magnitude. RAPT is a robust block that can easily be employed for virtually all samples containing systems of half-integer quadrupolar nuclei. On the other hand application of CPMG is useful mostly when inhomogeneous decay of nuclear magnetization under observation is much faster than the homogeneous one or when details about second-order quadrupolar lineshapes are not very important. Resolution of a robust and efficient 2Q homonuclear correlation experiment can be tremendously improved by a split-t_1 2Q6Q homonuclear correlation experiment. The experiment removes second-order quadrupolar line broadening and yields isotropic spectra along the indirectly detected dimension. Its performance was successfully demonstrated on two sodium containing samples, Na_2SO_4 and Na_2HPO_4. In Na_2HPO_4 5 out of 6 predicted correlation peaks could be detected. The 2Q6Q experiment is much less efficient than the related 2Q experiment, and also amplitudes of correlation peaks within 2Q6Q two-dimensional spectra depend much more on the magnitude of quadrupolar coupling constants than they do in 2Q spectra. Nevertheless, application of higher RF fields (so far only RF fields of up to 60 kHz were used) could certainly enhance the efficiency of the experiment and reduce its sensitivity to the magnitude of quadrupolar coupling. The 2Q6Q homonuclear correlation experiment could then be a valuable tool for studying dipolar couplings in systems of half-integer quadrupolar nuclei, in which central-transition signals broadened by the second-order quadrupolar anisotropy overlap severely.

Acknowledgments

Slovenian Ministry of Education, Science, and Sport is acknowledged for the financial support through research projects J1-6350-0104-04 and P1-0021-0104.

References

[1] G.E. Maciel, High-resolution nuclear magnetic-resonance of solids, Science 226 (1984) 282–288.
[2] E. Oldfield, R.J. Kirkpatrick, High-resolution nuclear magnetic-resonance of inorganic solids, Science 227 (1985) 1537–1544.
[3] L. Frydman, J.S. Harwood, Isotropic spectra of half-integer quadrupolar spins from bidimensional magic-angle-spinning NMR, J. Am. Chem. Soc. 117 (1995) 5367–5368.
[4] Z.H. Gan, Isotropic NMR spectra of half-integer quadrupolar nuclei using satellite transitions and magic-angle spinning, J. Am. Chem. Soc. 122 (2000) 3242–3243.
[5] G. Mali, F. Taulelle, Detecting proximities between quadrupolar nuclei by double-quantum NMR, Chem. Commun. (2004) 868–869.
[6] G. Mali, G. Fink, F. Taulelle, Double-quantum homonuclear correlation magic angle sample spinning nuclear magnetic resonance spectroscopy of dipolar-coupled quadrupolar nuclei, J. Chem. Phys. 120 (2004) 2835–2845.
[7] N.C. Nielsen, H. Bildsoe, H.J. Jakobsen, M.H. Levitt, Double-quantum homonuclear rotary resonance—efficient dipolar recovery in magic-angle-spinning nuclear-magnetic-resonance, J. Chem. Phys. 101 (1994) 1805–1812.
[8] Personal correspondence with F. Taulelle.
[9] S.P. Brown, S.J. Heyes, S. Wimperis, Two-dimensional MAS multiple-quantum NMR of quadrupolar nuclei, removal of inhomogeneous second-order broadening, J. Magn. Reson. Ser. A 119 (1996) 280–284.
[10] Z. Yao, H.T. Kwak, D. Sakellariou, L. Emsley, P.J. Grandinetti, Sensitivity enhancement of the central transition NMR signal of quadrupolar nuclei under magic-angle spinning, Chem. Phys. Lett. 327 (2001) 85–90.
[11] F.H. Larsen, H.J. Jakobsen, P.D. Ellis, N.C. Nielsen, QCPMG-MAS NMR of half-integer quadrupolar nuclei, J. Magn. Reson. 131 (1998) 144–147.
[12] D. Massiot, F. Fayon, M. Capron, I. King, S. Le Calve, B. Alonso, J.O. Durand, B. Bujoli, Z.H. Gan, G. Hoatson, Modelling one- and two-dimensional solid-state NMR spectra, Magn. Reson. Chem. 40 (2002) 70–76.

[13] M. Baldus, B.H. Meier, R.R. Ernst, A.P.M. Kentgens, H.M.Z. Altenschildesche, R. Nesper, Structure investigation on anhydrous disodium hydrogen phosphate using solid-state NMR and X-ray techniques, J. Am. Chem. Soc. 117 (1995) 5141–5147.
[14] M. Bak, J.T. Rasmussen, N.C. Nielsen, SIMPSON: a general simulation program for solid-state NMR spectroscopy, J. Magn. Reson. 147 (2000) 296–330.
[15] R. Lefort, J.W. Wiench, M. Pruski, J.P. Amoureux, Optimization of data acquisition and processing in Carr–Purcell–Meiboom–Gill multiple quantum magic angle spinning nuclear magnetic resonance, J. Chem. Phys. 116 (2002) 2493–2501.
[16] R.R. Ernst, G. Bodenhausen, A. Wokaun, Principles of Nuclear Magnetic Resonance in One and Two Dimensions, Clarendon Press, Oxford, 1987.
[17] G. Wu, D. Rovnyak, R.G. Griffin, Quantitative multiple-quantum magic-angle-spinning NMR spectroscopy of quadrupolar nuclei in solids, J. Am. Chem. Soc. 118 (1996) 9326–9332.
[18] T. Vosegaard, P. Florian, D. Massiot, P.J. Grandinetti, Multiple quantum magic-angle spinning using rotary resonance excitation, J. Chem. Phys. 114 (2001) 4618–4624.
[19] P.K. Madhu, A. Goldbourt, L. Frydman, S. Vega, Fast radio-frequency amplitude modulation in multiple-quantum magic-angle-spinning nuclear magnetic resonance: theory and experiments, J. Chem. Phys. 112 (2000) 2377–2391.
[20] A. Medek, J.S. Harwood, L. Frydman, Multiple-quantum magic-angle spinning NMR: a new method for the study of quadrupolar nuclei in solids, J. Am. Chem. Soc. 117 (1995) 12779–12787.
[21] M.J. Duer, A.J. Painter, Correlating quadrupolar nuclear spins: a multiple-quantum NMR approach, Chem. Phys. Lett. 313 (1995) 763–770.
[22] A.J. Painter, M.J. Duer, Double-quantum-filtered nuclear magnetic resonance spectroscopy applied to quadrupolar nuclei in solids, J. Chem. Phys. 116 (2002) 710–722.
[23] M.H. Levitt, P.K. Maduh, C.E. Hughes, Cogwheel phase cycling, J. Magn. Reson. 155 (2002) 300–306.
[24] C.E. Hughes, M. Carravetta, M.H. Levitt, Some conjectures for cogwheel phase cycling, J. Magn. Reson. 167 (2004) 259–265.
[25] A. Jerschow, R. Kumar, Calculation of coherence pathway selection and cogwheel cycles, J. Magn. Reson. 160 (2003) 59–64.